PHYSICAL REVIEW B VOLUME 2, NUMBER 8 15 OCTOBER 1970

Sublimation Pressures of Solid Ar, Kr, and Xe†

Charles W. Leming* and Gerald L. Pollack
Michigan State University, East Lansing, Michigan 48823
(Received 21 April 1970)

Results of an experiment to measure the sublimation pressures of Ar, Kr, and Xe over wide temperature and pressure ranges are presented. Data are reported from near the respective triple points to about (2.3×10^{-6} Torr, 25.506 K) for Ar; (2.1×10^{-4} Torr, 45.130 K) for Kr; (3.8×10^{-4} Torr, 70.075 K) for Xe. Pressures were measured with a Hg manometer, a McLeod gauge, and a calibrated Bourdon gauge. The data have been corrected for thermomolecular flow and streaming. Temperatures were measured with a N.B.S.-calibrated Pt resistance thermometer. The application of the law of corresponding states is investigated. Values for static lattice energy, geometric mean of the lattice vibrational spectrum, heat of sublimation, and lattice vibrational energy are calculated using theoretical sublimation pressure curves.

INTRODUCTION

Properties of the rare-gas solids have long created much interest because the nature of the attractive forces between atoms is simple and rather well understood.[1,2] These forces may be closely approximated as short-range pairwise additive central forces which have the same form for all the rare gases.[3] Many thermodynamic properties of these solids have been predicted on the basis of simple models. Deviations in the experimental data may be used to study such details as anharmonicity,[4,5] electron exchange,[6] and lattice defects.[7,8]

The purpose of our work is to provide accurate pressure data extending over several orders of magnitude for each gas. All measurements were made using the same apparatus and are thus particularly useful for a consistent corresponding states analysis of the reduced-pressure curves.

These data have been analyzed on the basis of vapor-pressure curves predicted by classical thermodynamics[9] and vapor-pressure curves predicted by lattice dynamical theory.[7] From this analysis we were able to calculate values for heats of fusion, vibrational energies, static lattice energies, and the geometric mean of the lattice vibrational spectra. The law of corresponding states has been applied to test the consistency of published potential parameters for Ar, Kr, and Xe.

This paper describes our experiment and calculations. Results of this experiment are reported in terms of parameters for vapor-pressure curves and also in tables of primary data. We hope these tables of data may be useful for analysis by other workers.[7]

EXPERIMENTAL

In order to perform this experiment over the wide pressure and temperature ranges desired, it was first necessary to construct a constant-temperature cryostat for use in the range 25–170 K. Heat input requirements were not so stringent as in the case of an adiabatic calorimeter so the cryostat design could be simplified. Figure 1 shows the basic construction of our cryostat.

The sample chamber within the copper block is connected to a glass gas-handling system and pressure-measuring device (not shown) by a $\frac{1}{4}$-in. -i.d. stainless-steel inlet tube. A stainless-steel outer jacket encloses the Cu block. Thermal contact between the sample chamber and the low-temperature bath is achieved with He exchange gas. Heat is distributed through the sample by means of four copper vanes.

For temperatures from 90–55 K, the apparatus was immersed in a liquid-oxygen bath whose temperature was controlled by pumping through an automatic pressure regulator. This provides a

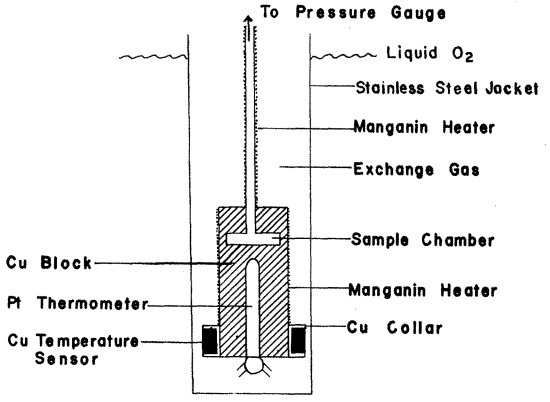

FIG. 1. Sectional view of sublimation pressure apparatus.

convenient constant-temperature bath which allows good temperature control with only small amounts of electrical heating. When temperatures higher than the bath temperature are required, the exchange gas is pumped away and the Cu block is heated. For temperatures below 55 K, the apparatus was suspended above a He bath while cold vapor was evaporated from the bath and pumped around the outer stainless-steel jacket.

Accurate temperature regulation of the Cu block was achieved using a commercial ac bridge temperature controller.[10] A noninductive resistive temperature sensor of Cu wire wound on a Cu collar around the block served as the temperature-sensitive arm of the bridge. Although such a thermometer is not reproducible over several cooling cycles, it was sufficiently stable over a single cycle to provide reliable control.

The output of the controller was applied to a manganin heater wound directly on the Cu block. An independently controlled heater was wound on the stainless-steel inlet tube. With this system, we could control the sample temperature to ± 1 mdeg K for the length of time necessary to take measurements, and to ± 5 mdeg K for longer periods of time.

Thermal gradients in the Cu block and in the sample were investigated. We admitted exchange gas to the vacuum space and electrical heating was simultaneously increased to maintain a constant temperature. The vapor-pressure reading was monitored in order to be sure no change in sample temperature occurred when heater power was increased. Small thermal gradients of about 2 mdeg K were observed at the maximum power input available to the heater. Consequently, the heater was never operated over about 10% of maximum power while taking data. Thermal gradients due to the heater on the inlet tube were similarly investigated but none were detected.

Temperature was measured on two different capsule-type Pt resistance thermometers imbedded in the Cu block. Thermal contact between the Cu block and the resistance thermometers was through a thin layer of Apiezon-L vacuum grease. The thermometers were calibrated by the National Bureau of Standards using the 1968 International Practical Temperature Scale. One of the thermometers was calibrated above 90 K and the other below 92 K. The data remained consistent in the overlapping region. Thermometer resistance was measured on a Leeds and Northrup calibrated K-5 potentiometer using the standard single-potentiometer technique.[11]

Careful temperature measurement and control were necessary while condensing the sample in order to avoid condensation of gases on the walls of the inlet tube. The entire system was first heated to a high enough temperature that gas would not condense. The temperature of the Cu block was then slowly lowered so that the block was the coldest part of the system. Condensation was then limited to the sample chamber by keeping the gas pressure near the equilibrium vapor pressure as the sample was formed. Samples were condensed at various temperatures and no change in vapor pressure could be measured due to the temperature range in which the sample was condensed. No attempt was made to grow single crystals or control grain size.

After a solid sample with a volume of approximately 0.8 cm^3 was formed, the system was checked for parasitic condensation on the inlet tube. This was done by maintaining the sample-chamber temperature constant and increasing the heater current to the inlet tube. If the pressure was observed to increase under these conditions, the sample was evaporated and replaced.

Pressure measurements above 1 Torr were made on a Texas Instruments quartz spiral Bourdon gauge. This gauge was equipped with high-sensitivity elements capable of detecting pressure changes of less than 1 mTorr. The elements were calibrated to about ± 0.02 Torr against a Hg manometer read with a Wild cathetometer. The manometer readings were corrected to 0° C density of Hg and standard gravity ($g = 980.665$ cm/sec^2). Corrections were also applied to account for capillary depression in the Hg manometer.[12]

Pressures below 1 Torr were measured using a McLeod gauge. Near 1 Torr the gauge readings have an estimated accuracy of 1%. Near 10^{-4} or 10^{-5} Torr, the lower usable limit of the gauge, the gauge readings have an estimated accuracy of 5%. All McLeod readings were corrected for Hg streaming.[13] Readings below 1 Torr were also corrected for thermal transpiration, as described by Takaishi and Sensui.[14] This latter correction was adequate down to pressures of about 0.1 Torr, but for lower pressures deviations appeared which could only be attributed to the correction itself.

Samples were condensed from Matheson research-grade gases. Mass-spectrometer analysis provided with the samples listed the main impurities in the Ar as 3.5 ppm H_2O and 3.0 ppm O_2. The main impurity in the Kr sample was 13 ppm Xe and the main impurity in the Xe sample was 18 ppm Kr. More impurities were probably present because of outgassing from the walls of the storage cylinders.

At high pressures, these impurity levels have little effect on the sublimation pressure, but at low pressures, the partial pressures of the relatively volatile impurities can easily approach the partial pressure of the primary gas component. In

order to purify the gas further, we preferentially distilled the samples *in situ* by expanding the vapor phase into our gas-handling system. Data were taken on the purified sample after such distillations caused no change in the measured sublimation pressure.

During the course of measurements, contamination of the sample was observed due to outgassing from the walls of the apparatus. This outgassing was decreased by building the room-temperature part of the system from stainless steel and glass. Gases adsorbed on these surfaces were removed by heating the system and evacuating the purged gases until no pressure increase in the system could be seen. Following this degassing technique, the system could be sealed for several hours before any pressure increases were detectable.

RESULTS

The measured pressure and temperature points are presented in Table I. Figures 2–4 of the text show the measured sublimation pressures P plotted as functions of temperature T.

Law of Corresponding States

The sublimation pressure curves of rare-gas solids may be related by means of the law of corresponding states.[15] This law predicts similarities in the form of the equation of state of substances whose binding potentials may be written as a sum of identical expressions $\phi(r_{ik})$.[16,17] These binding potentials must only depend on the separation r_{ik} between pairs of molecules and must have the form

$$\phi(r) = \epsilon f(r/\sigma) .$$

In this expression ϵ and σ are the characteristic energy and length for each potential and $f(r/\sigma)$ is a dimensionless function which has the same form for each molecule. No specific form of $f(r/\sigma)$ is required for this law to apply.

If these conditions are met, the thermodynamic properties should all be functions of the dimensionless reduced variables P^*, V^*, T^*, and Λ^* which are defined as follows:

$$P^* = P\sigma^3/\epsilon, \quad V^* = V/N\sigma^3,$$

$$T^* = kT/\epsilon, \quad \Lambda^* = h/\sigma\,(m\epsilon)^{1/2} .$$

The parameter Λ^* gives the relative size of quantum effects.

It is further expected that the reduced sublimation pressure curves for rare gases should follow this law and yield reduced-pressure curves which increase monotonically with increasing Λ^*, i.e., with decreasing atomic mass.[18] When accepted parameters for the Mie–Lennard-Jones potential and the Morse potential are used to calculate the

TABLE I. Measured pressure and temperature points.

Ar		Kr		Xe	
Press. (Torr)	Temp. (K)	Press. (Torr)	Temp. (K)	Press. (Torr)	Temp. (K)
561.099	84.495	505.261	114.914	505.969	158.710
538.557	84.128	502.293	114.855	496.632	158.458
513.970	83.730	482.453	114.457	486.381	158.170
492.247	83.412	460.901	114.010	465.899	157.588
464.519	82.994	441.980	113.608	444.649	156.972
448.290	82.742	421.227	113.141	424.359	156.354
443.067	82.661	417.699	113.072	403.954	155.706
420.063	82.266	400.137	112.649	383.428	155.028
385.901	81.666	393.148	112.494	373.930	154.709
358.409	81.155	380.794	112.179	363.577	154.342
340.153	80.797	370.278	111.939	355.436	154.058
313.180	80.238	359.921	111.650	342.665	153.582
299.849	79.947	351.269	111.433	335.974	153.341
284.865	79.647	341.909	111.169	322.624	152.820
271.425	79.287	327.079	110.772	316.179	152.579
261.737	79.038	318.285	110.512	302.091	151.999
254.242	78.858	310.807	110.305	295.350	151.727
236.758	78.399	300.348	109.982	284.928	151.282
218.673	77.892	237.134	109.600	281.254	151.114
204.450	77.463	283.954	109.476	273.829	150.798
189.298	76.984	263.805	108.828	270.013	150.607
173.501	76.444	261.753	108.746	268.649	150.561
167.508	76.226	249.681	108.341	252.950	149.831
159.117	75.916	241.268	108.029	250.344	149.692
145.576	75.383	238.618	107.926	249.147	149.645
128.462	74.613	209.386	107.799	241.695	149.296
119.122	74.286	222.243	107.317	235.097	148.949
114.188	74.000	221.013	107.279	231.717	148.781
98.050	73.138	209.386	106.799	230.188	148.684
90.947	72.719	193.818	106.138	213.153	147.800
79.972	72.013	181.424	105.588	205.518	147.350
73.900	71.589	175.569	105.304	196.376	146.840
68.564	71.191	168.667	104.978	187.374	146.271
62.115	70.673	160.055	104.540	181.283	145.921
57.647	70.286	156.598	104.370	170.785	145.211
53.339	69.886	147.423	103.886	166.702	144.965
53.106	69.867	128.521	102.776	154.186	144.088
49.988	69.560	123.549	102.463	153.757	144.058
46.716	69.219	119.813	102.226	139.989	143.018
41.593	68.643	113.961	101.834	138.631	142.831
37.246	68.106	105.260	101.224	128.865	142.115
36.375	67.992	98.954	100.749	118.179	141.183
34.477	67.735	92.135	100.213	100.106	139.419
32.091	67.397	82.361	99.378	96.094	138.992
28.104	66.777	73.122	98.506	90.905	138.418
26.967	66.586	62.813	97.418	84.552	137.680
24.661	66.178	56.989	96.734	81.521	137.310
22.703	65.802	51.082	95.974	74.512	136.409
19.304	65.080	43.539	94.889	74.491	136.400
17.436	64.637	39.466	94.238	67.318	135.403
16.172	64.312	21.663	90.450	65.980	135.198
14.199	63.754	20.965	90.250	64.131	134.931
13.547	63.556	20.202	90.029	58.299	134.006
10.636	62.552	19.003	89.660	57.887	133.928
8.132	61.521	18.953	89.644	52.315	132.972
4.703	59.443	17.324	89.114	50.895	132.699
3.983	58.808	14.773	88.189	47.631	132.088
3.243	58.095	13.995	87.877	44.742	131.498

TABLE I. (*continued*).

Ar Press. (Torr)	Ar Temp. (K)	Kr Press. (Torr)	Kr Temp. (K)	Xe Press. (Torr)	Xe Temp. (K)
2.121	56.608	12.781	87.366	42.894	131.117
0.601	52.488	12.709	87.328	39.719	130.405
0.204	50.018	11.733	86.882	38.325	130.088
0.0675	47.845	10.923	86.468	35.224	129.326
0.0660	47.739	10.044	86.027	34.664	129.176
0.0262	45.929	8.820	85.316	31.178	128.240
0.0218	45.492	7.754	84.635	30.294	127.978
0.0158	44.807	7.065	84.138	28.910	127.577
0.0108	44.015	6.733	83.879	28.844	127.5430
7.5×10^{-3}	43.160	5.893	83.215	26.533	126.822
6.0×10^{-3}	42.769	5.387	82.761	26.367	126.764
3.8×10^{-3}	41.871	4.549	81.896	25.702	126.538
8.2×10^{-4}	38.707	3.604	80.746	24.894	126.279
2.2×10^{-4}	36.803	3.181	80.156	23.177	125.686
7.0×10^{-5}	34.977	2.525	79.054	22.829	125.544
3.4×10^{-5}	33.930	2.110	78.199	20.236	124.530
1.5×10^{-5}	32.146	1.962	77.853	20.168	124.520
8.7×10^{-6}	30.400	1.554	76.773	18.011	123.585
5.0×10^{-6}	29.099	1.133	75.278	17.567	123.358
3.5×10^{-6}	27.601	0.841	74.027	15.988	122.613
3.4×10^{-6}	27.525	0.523	72.279	15.575	122.375
2.7×10^{-6}	26.065	0.389	71.057	14.222	121.671
2.3×10^{-6}	25.506	0.295	70.342	13.940	121.485
		0.186	68.663	12.475	120.640
		0.140	68.070	12.227	120.448
		0.131	67.589	10.963	119.599
		0.092	66.822	9.661	118.619
		0.0879	66.590	3.594	111.004
		0.0619	65.675	2.859	109.519
		0.0608	65.620	2.323	108.183
		0.0467	64.909	1.809	106.962
		0.0337	64.084	1.383	105.018
		0.0231	63.138	1.034	103.316
		0.0172	62.152	0.767	101.672
		0.0136	61.244	0.367	97.826
		0.0119	61.128	0.246	95.935
		8.0×10^{-3}	60.122	0.162	94.136
		7.5×10^{-3}	59.727	0.132	93.106
		4.6×10^{-3}	58.304	0.106	92.117
		3.5×10^{-3}	57.565	0.0843	91.759
		2.1×10^{-3}	56.297	0.0522	89.851
		1.7×10^{-3}	55.415	0.0321	88.013
		1.0×10^{-3}	54.380	0.0205	86.253
		8.6×10^{-4}	53.467	0.0179	85.963
		5.2×10^{-4}	51.961	0.0136	84.830
		3.0×10^{-4}	49.259	0.0108	83.646
		2.1×10^{-4}	46.017	9.0×10^{-3}	83.020
		2.1×10^{-4}	45.130	7.2×10^{-3}	81.923
				5.6×10^{-3}	81.528
				4.8×10^{-3}	80.982
				4.3×10^{-3}	80.806
				3.4×10^{-3}	79.587
				2.9×10^{-3}	78.865
				2.3×10^{-3}	78.082
				1.6×10^{-3}	76.474
				1.4×10^{-3}	76.034
				8.1×10^{-4}	74.054
				6.0×10^{-4}	72.522
				4.7×10^{-4}	71.372
				3.8×10^{-4}	70.075

reduced variables, the reduced-pressure curves are found to deviate from the expected order. This effect is shown in Fig. 5, for which we used the potential parameters given by Horton[3] for the all-neighbor Mie–Lennard-Jones potentials. For Fig. 5, σ was chosen according to the definition given by De Boer, [16] $\phi(r=\sigma)=0$.

The curves on Fig. 5 show approximately the expected behavior, except that the Kr and Xe curves are interchanged. This effect has been observed in other properties and by other investigators.[15,18] The reasons for this deviation are not clear. Possibly, the actual potential deviates from any of the analytic potentials proposed so far, or the basic assumptions of pairwise additive forces, which only depend on the separation distance, are not met.

Static Lattice Energy

By fitting our data to the theoretical vapor-pressure curve derived by Salter, [7] we obtained values for static lattice energy and geometric mean of the lattice vibrational spectrum. These appear in Table II. Assuming perfect crystal structure, quasiharmonic lattice vibrations, and an almost ideal vapor; a direct application of statistical

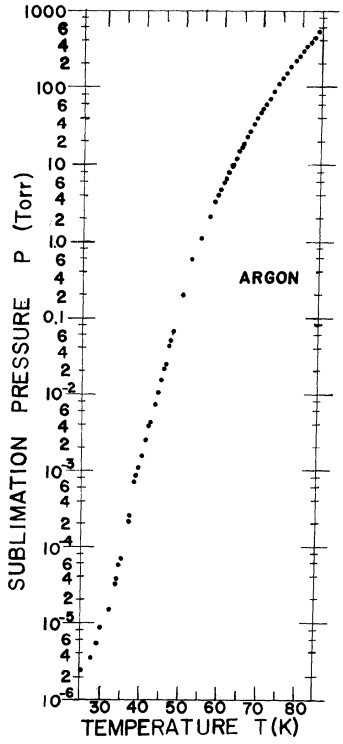

FIG. 2. Sublimation pressure of solid Ar as a function of temperature. The data level off at low temperatures because of the presence of impurities.

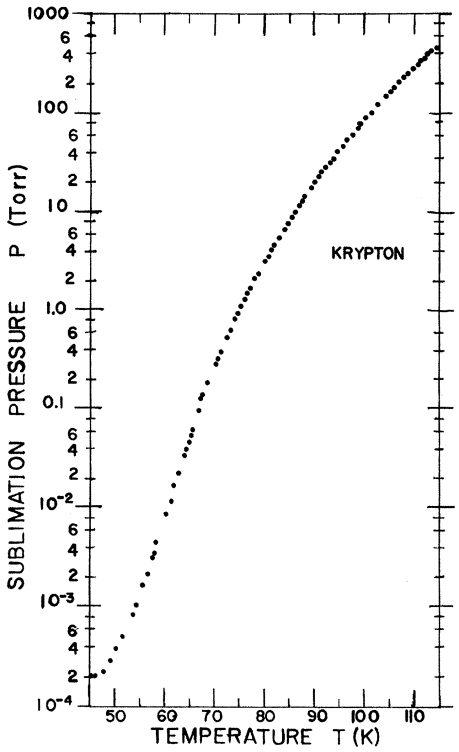

FIG. 3. Sublimation pressure of solid Kr as a function of temperature.

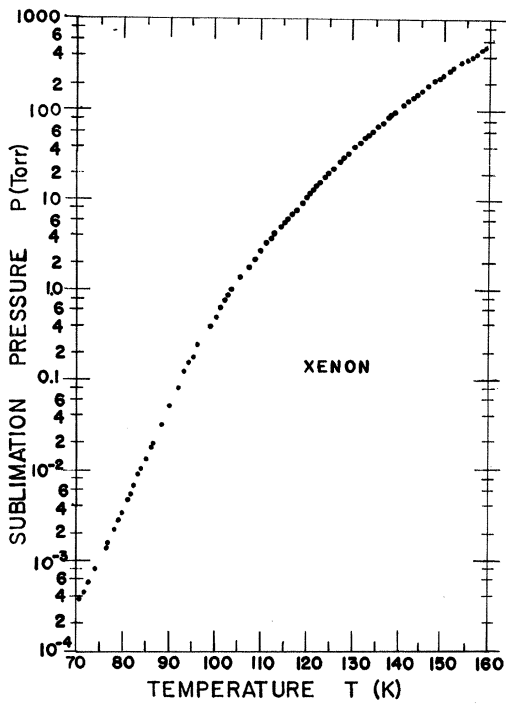

FIG. 4. Sublimation pressure of solid Xe as a function of temperature.

mechanics yields the vapor-pressure curve[7]

$$\ln P = -\tfrac{1}{2}\ln T + a/T + b\ ,$$

where (1)

$$a = \frac{U}{Nk}\ , \quad b = 3\ln\omega_g + \tfrac{1}{2}\ln\left[\left(\frac{m^3}{2\pi}\right)\frac{1}{k}\right].$$

In this equation, $-U$ is the static lattice energy, which at 0 K is related to the heat of sublimation L and the zero-point energy E_z by $-U(0\,\mathrm{K}) = L(0\,\mathrm{K}) + E_z(0\,\mathrm{K})$. The geometric mean of the lattice vibrational spectrum ω_g is defined as

$$\omega_g = \left(\prod_{i=1}^{3N}\omega_i\right)^{1/3N}. \tag{2}$$

Equation (1) is applicable for temperatures greater than one-half the Debye temperature and temperatures low enough that the effects of anharmonicity and vacancies are not important.

The effect of vacancy formation can be taken into account by considering the change in Gibbs free energy of the crystal due to vacancy formation. When this is done, the equation corresponding to Eq. (1) is

$$\ln P = \tfrac{1}{2}\ln T + a/T + b - e^{-gs/kT}. \tag{3}$$

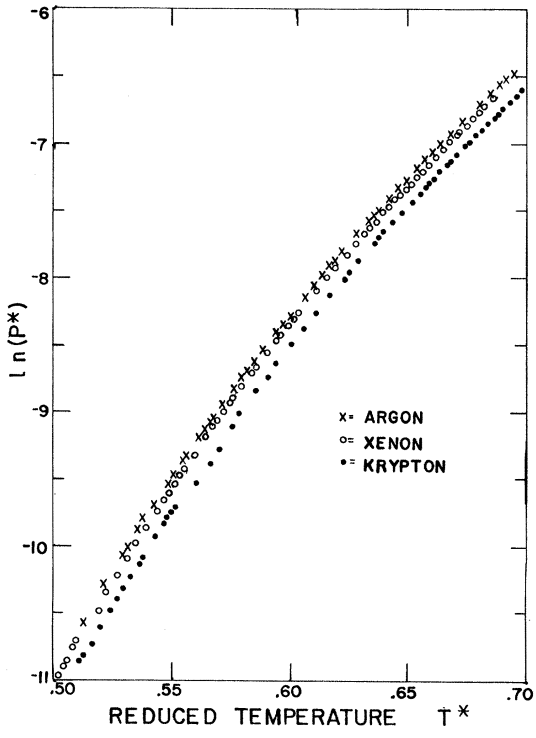

FIG. 5. Reduced sublimation pressure P^* as a function of reduced temperature T^* for Ar, Kr, and Xe.

TABLE II. Static lattice energies U and geometric mean of the lattice vibrational spectrum ω_g calculated from our data using Eq. (1) are presented in the fourth and fifth columns. The sixth and seventh columns show the parameters corrected for vacancy formation using Eq. (3). Temperature intervals and the mean temperature used for calculation are presented in the second and third columns.

Gas	Temp. range (K)	Mean temp. (K)	Uncorrected		Corrected	
			$-U$ (cal/mole)	ω_g (10^{12} sec^{-1})	$-U$ (cal/mole)	ω_g (10^{12} sec^{-1})
Ar	84.5–78.0	81.2	1964	6.60	1978	6.82
Ar	78.0–72.0	75.0	1985	6.91	1994	7.07
Ar	72.0–66.0	69.0	1976	6.77	1979	6.82
Ar	66.0–54.0	60.0	1974	6.73	1976	6.76
Ar	54.0–40.0	47.0	2108	9.97	2108	9.97
Kr	115.0–107.0	111.0	2756	5.23	2773	5.38
Kr	107.0–98.4	102.8	2754	5.22	2762	5.29
Kr	98.4–90.2	94.3	2768	5.34	2772	5.38
Kr	90.2–73.8	82.0	2719	4.85	2738	5.06
Kr	73.8–54.7	63.2	2862	6.48	2860	6.42
Xe	162.0–150.2	156.1	3841	4.57	3864	4.71
Xe	150.2–139.0	144.6	3833	4.53	3838	4.57
Xe	139.0–127.0	133.0	3837	4.55	3842	4.58
Xe	127.0–104.0	115.5	3768	4.15	3686	3.71
Xe	104.0–76.2	90.1	4029	6.51	3988	5.96

In Eq. (3), a and b are defined as in Eq. (1) and g_S is the Gibbs free energy for vacancy formation. Values used for g_S for Ar and Kr are those found by Beaumont *et al.*[19] These values estimated from vacancy effects on specific-heat data are for Ar,

$$e^{-g_S/kT} = 30\, e^{-644.2\,K/T} ,$$

and for Kr,

$$e^{-g_S/kT} = 30\, e^{-890.8\,K/T} .$$

No vacancy concentration measurements were available for Xe, so the value of g_S for Xe was estimated by using the law of corresponding states. The reduced value of g_S for Xe was assumed to be equal to the average reduced values of g_S for Ar and Kr. Using Horton's parameters[3] as before, we find for Xe, $e^{-g_S/kT} = 30\, e^{-(1248\ \mathrm{K})/T}$.

The quantities U and ω_g depend on volume, so that the calculated values change with temperature. Different temperature intervals were used for fitting the data to Eqs. (1) and (3) and the values reported refer to a volume corresponding to the center of each interval. The temperature intervals used were chosen to correspond to the same reduced temperature intervals for each gas.

Heat of Sublimation

The data were also fitted to the Clausius-Clapeyron equation[20] to obtain values for the heat of sublimation. Results of this analysis appear in Table III.

The integrated form of the Clausius-Clapeyron equation can be written as

$$\ln P = a/T + b ,$$

where

$$a = -\frac{h_S - h_G}{R(1 - v_S/v_G + BP/RT)} . \qquad (4)$$

The heat of sublimation L is given by the difference in specific enthalpies of the gas and the solid $h_G - h_S$. Heat of sublimation depends on vibrational energy and volume, so that a varies with temperature. The same temperature intervals used in Table II were used for the least-squares fit of the date to Eq. (4). Values for the second virial coefficient B were obtained from an extrapolation of reduced curves.[21] The specific volumes of the solid v_S were obtained from density curves.[2]

For comparison with our values, some values for a and b found by other workers follow: For the temperature interval 83.6–66.1 K, Flubacher *et al.*[22] found $a = 953.897$, $b = 17.628\,36$ for Ar. For the temperature interval 115.8–83.3 K, Beaumont *et al.*[19] found $a = 1127.58$, $b = 16.046\,25$ for Kr. For the temperature interval 161–110 K, Freeman and Halsey[23] found $a = 1840.0$, $b = 16.972$ for Xe. Our parameters calculated for Kr differ significantly from those found by Beaumont *et al.*,[19] but are closer to the parameters $a = 1334.6$, $b = 17.833$ found earlier by Freeman and Halsey[23] for the temperature interval 115–80 K.

Lattice Vibrational Energy

The lattice vibrational energy E_{vib} may now be

TABLE III. Values of parameters a and b of Eq. (4) for Ar, Kr, and Xe are given in the fourth and fifth columns. The sixth column shows calculated values of the heat of sublimation L. Temperature intervals and the mean temperature used for calculation are presented in the second and third columns.

Gas	Temp. range (K)	Mean temp. (K)	$-a$	b	L (cal/mole)
Ar	84.5–78.0	81.2	946.35	17.5408	1852
Ar	78.0–72.0	75.0	962.22	17.7428	1900
Ar	72.0–66.0	69.0	960.59	17.7214	1904
Ar	66.0–54.0	60.0	963.39	17.7627	1914
Ar	54.0–40.0	47.0	1038.03	19.0767	2062
Kr	115.0–107.0	111.0	1332.30	17.8184	2612
Kr	107.0–98.4	102.8	1334.63	17.8413	2636
Kr	98.4–90.2	94.3	1346.76	17.9656	2670
Kr	90.2–73.8	82.0	1330.73	17.7765	2644
Kr	73.8–54.7	63.2	1399.08	18.5731	2780
Xe	162.0–150.2	156.1	1856.41	17.9236	3480
Xe	150.2–139.0	144.6	1857.02	17.9276	3596
Xe	139.0–127.0	133.0	1860.70	17.9513	3661
Xe	127.0–104.0	115.5	1836.37	17.7526	3632
Xe	104.0–76.2	90.1	1960.37	18.9607	3895

calculated using the relation

$$E_{\text{vib}} = -U - L + P(v_G - v_S) . \quad (5)$$

The specific volumes used are the same as those used to calculate the heat of sublimation.[2] The results are given in Table IV.

DISCUSSION

As is evident from Figs. 2–4, the accuracy of our data at low temperatures and low pressures is limited by the impurities present. For each gas, the pressure curves began to flatten when the impurity concentrations for the vapor phase became large compared to the concentration of the primary gas.

These curves were reproducible for different gas samples and different runs. This indicates that the impurities were present in the samples and were not evolved from the walls of the system. Assuming the impurities present are noncondensable gases such as helium, we estimate the impurity concentrations to be about 0.2 ppm for Ar, 13 ppm for Kr, and 10 ppm for Xe. This estimate of noncondensable impurities is probably accurate for Ar, but may not be so reliable for Kr and Xe because the partial pressure of condensed impurities is higher for these gases.

A further source of inaccuracy is the correction made for thermomolecular flow. Even though our gas inlet tube was of relatively large diameter ($\frac{1}{4}$ in. i.d.), this correction became important at low pressures. The correction was obtained by application of an empirical equation.[14] Most of the data which were originally used to fix the parameters of this equation were from higher temperatures than those used in our experiment. Our analysis indicates a large overcorrection as shown by anomalous values for static lattice energy and heat of sublimation for low reduced temperatures $T^* \simeq 0.5$. In order to make low-temperature data more meaningful, both an improved correction for thermomolecular flow as well as higher-purity gases are required.

TABLE IV. Vibrational energies calculated from Eq. (5) for Ar, Kr, and Xe are presented in the fourth column. The third column gives the temperature for which these values of vibrational energy were found. Data from the temperature intervals shown in the second column were used for the calculations.

Gas	Temp. range (K)	Mean temp. (K)	Vibrational energy (cal/mole)
Ar	84.5–78.0	81.2	285
Ar	78.0–72.0	75.0	243
Ar	72.0–66.0	69.0	213
Ar	66.0–54.0	60.0	181
Ar	54.0–40.0	47.0	139
Kr	115.0–111.0	111.0	381
Kr	107.0–98.4	102.8	331
Kr	98.4–90.2	94.3	288
Kr	90.2–73.8	82.0	258
Kr	73.8–54.7	63.2	205
Xe	162.0–150.2	156.1	693
Xe	150.2–139.0	144.6	529
Xe	139.0–127.0	133.0	445
Xe	127.0–104.0	115.5	281
Xe	104.0–76.2	90.1	272

†Work supported by U. S. Atomic Energy Commission.

*This article is based on a thesis submitted in partial fulfillment for the degree of Doctor of Philosophy from Michigan State University, 1970. Present address: Physics Department, Henderson State College, Arkadelphia, Ark. 71923.

[1]E. R. Dobbs and G. O. Jones, Rept. Progr. Phys. 20, 516 (1957).

[2]G. L. Pollack, Rev. Mod. Phys. 36, 748 (1964).

[3]G. K. Horton, Am. J. Phys. 36, 93 (1968).

[4]M. L. Klein, J. Chem. Phys. 41, 749 (1964).

[5]M. L. Klein and J. A. Reissland, J. Chem. Phys. 41, 2773 (1964).

[6]L. Jansen, Phil. Mag. 8, 1305 (1965).

[7]L. S. Salter, Trans. Faraday Soc. 59, 657 (1963).

[8]D. L. Losee and R. O. Simmons, Phys. Rev. Letters 18, 451 (1967).

[9]R. Becker, *Theorie der Wärme* (Springer, Berlin, 1953), p. 38.

[10]F. B. Rolfson, in *Temperature, Its Measurement and Control in Science and Industry*, edited by A. I. Dahl (Rheinhold, New York, 1962), Vol. 3, part 2, p. 787.

[11]H. L. Daneman and G. C. Mergner, Instrum. Technol. 14, 51 (1967).

[12]J. Kistemaker, Physica 11, 277 (1945).

[13]A. E. deVries and P. K. Rol, Vacuum 15, 135 (1965).

[14]T. Takeishi and Y. Sensui, Trans. Faraday Soc. 59, 2503 (1963).

[15]G. L. Pollack, Phys. Rev. A 2, 38 (1970).

[16]J. E. DeBoer, Physica 14, 139 (1948).

[17]J. E. DeBoer and B. S. Blaisse, Physica 14, 149 (1948).

[18]G. Boato and G. Casanova, Physica 27, 571 (1961).

[19]R. H. Beaumont, H. Chihara, and J. A. Morrison, Proc. Phys. Soc. (London) 78, 1462 (1961).

[20]Y. Larher, J. Chim. Phys. 65, 114 (1968).

[21]L. Bewilogua and C. Gladun, Contemp. Phys. 9, 277 (1968).

[22]P. Flubacher, A. J. Leadbetter, and J. A. Morrison, Proc. Phys. Soc. (London) 78, 1449 (1961).

[23]M. P. Freeman and G. D. Halsey, Jr., J. Phys. Chem. 60, 1119 (1956).

PHYSICAL REVIEW B VOLUME 2, NUMBER 8 15 OCTOBER 1970

V_3 Band in LiF†

M. R. Mayhugh and R. W. Christy
Dartmouth College, Hanover, New Hampshire 03755
(Received 7 April 1970)

An optical absorption band is produced at 113 nm (11.0 eV) in both pure and Mg-doped LiF by irradiation with x rays at room temperature. This band, which appears to be intrinsic like the F band, is identified as the V_3 band. Its peak-wavelength position follows the same dependence on anion radius as has been found previously for alkali chlorides, bromides, and iodides.

Ionizing radiation produces in pure alkali halide crystals a defect center which absorbs light in the wavelength range where the unirradiated crystal is transparent – the F center. This center consists of an electron trapped at an anion vacancy. The irradiation must also produce a complementary trapped-hole center. When the irradiation is near room temperature, this is thought to be the V_3 center, [1] which absorbs light to the short-wavelength side of the F band, near the fundamental absorption edge of the perfect crystal. The V_3 absorption band has been studied in some detail in KCl, [2–7] KBr, [2–4] and RbCl. [4] The preponderance of this evidence suggests that the V_3 center is a molecular halogen center. [1,8]

The F center and some other electron and hole centers in LiF are well known, but the V_3 center has not yet been identified. Extrapolation of regularities found in other alkali halides[1] leads to the expectation that it should lie near 11 eV, just before the fundamental absorption edge. Previous investigations of the vacuum-uv region of irradiated LiF have indeed shown a peak at this location, [9,10] but it was not identified as the V_3 band. Our purpose is to discuss some new measurements and argue that this peak is, in fact, the V_3 band in LiF.

Optical-absorption measurements were made on both pure and doped LiF crystals in the range from 2 to 12 eV, using a Unicam SP-700 spectrophotometer and a McPherson vacuum-uv monochromator, model No. 235. Details of the operation of the latter instrument are reported elsewhere. [11] In the V_3-band region it was important to correct for stray light, [12] particularly in the doped crystals which had a large impurity absorption before irradiation. The pure LiF crystals were obtained from Harshaw Chemical Co. in 1968, and the impure ones in 1954. The latter contain of the order of 100 ppm Mg, [13] compared to about 1 ppm in the former.

To summarize some results which are described in more detail elsewhere, [11] irradiation of a pure LiF crystal at room temperature produces the F band at 250 nm and the band at 113 nm (11.0 eV) which we shall identify as the V_3 [see Fig. 1 (a)]. Irradiation of the Mg-doped crystal produces these same two bands, and, in addition, some electron